Proceedings of the 1996 IEEE
International Conference on Robotics and Automation
Minneapolis, Minnesota - April 1996

Sonar Sensing Strategies

Thomas C. Henderson, Beat Bruderlin, Mohamed Dekhil, Larry Schenkat, and Larkin Veigel*

Department of Computer Science
University of Utah
Salt Lake City, Utah 84112

Abstract

We develop theoretical and practical techniques to recover the pose of planar surfaces with minimal sensor readings and motion. A proof is given that two sonar readings suffice to precisely locate a single planar surface that returns the sonar's signal. An implementation is described that takes into account the physical restrictions on actual Polaroid sensors and experiments are described based on actual Polaroid sensor data.

1 Introduction

Many authors have written about the use of sonar sensors for mapping indoor environments [2, 3, 4, 10]. Others have addressed special sensor configurations to disambiguate walls from corners and edges [1, 7, 11], or have shown the minimum number and arrangement of sonar sensors to detect obstacles[8, 9]. However, no one has addressed the optimal pose recovery of planar surfaces in sonar data. In this paper, we address the simplest version of the k-wall/m-sonar (kWmS) problem:

> **Problem:** Given m sonar transmitter/receiver sensors situated on a circular ring placed in a k wall enclosure, what is the optimal sensing strategy to determine the pose of the k walls?

The sonar sensor is assumed to have a non-zero beam spread (e.g., 22.5 degrees for a Polaroid sensor), and optimal is defined in terms of the recovery of the wall's pose with the minimum number of sensors used and moves made.

We consider the 1W1S problem in the plane (of the sonar ring) here and show that two independent sonar readings suffice to determine the pose of any wall that returns the sonar signals. (Walls show up as lines in this analysis.) This approach works better in practice than other methods currently in use.

The 1W1S Problem

Suppose we are given a single sonar located at s on a circular platform of radius a as shown in Figure 1, and that it indicates a return at range r. The sensor is assumed to have a beam spread 2σ, and to reflect back a signal incident to a surface at any angle (the fact that there is in practice a minimum incident angle that gives a reflection will be accounted for later). Furthermore, assume that there is only one wall in the vicinity of the sonar and it reflects a signal (i.e., it intersects the sonar wedge).

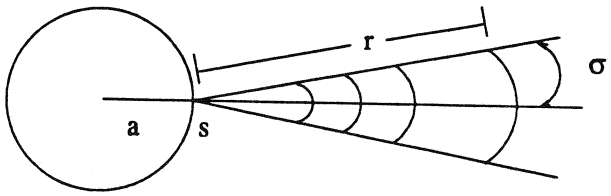

Figure 1: Single Sonar Beam

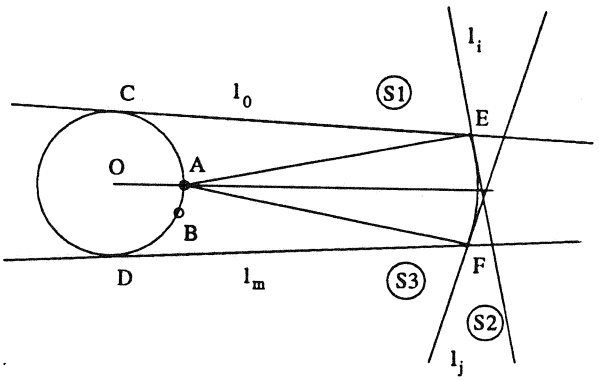

Figure 2: Qualitative Line Sets

Then Figure 2 shows the three qualitatively different sets of possible lines that could have produced a range reading of r. The qualitative line sets are:

1. $S1$: The set of lines found by rotating l_0 about E into l_i.
2. $S2$: The set of lines found by sliding the tangent line along the circular arc EF from l_i to l_j.
3. $S3$: The set of lines found by rotating l_j about F into l_m.

We will show that the line which caused the range return value of r can be disambiguated by taking one more sonar

*This work was supported in part by the Advanced Research Projects Agency under Army Research Office grant number DAAH04-93-G0420, and NSF grant CDA 9024721. All opinions, findings, conclusions or recommendations expressed in this document are those of the author and do not necessarily reflect the views of the sponsoring agencies.

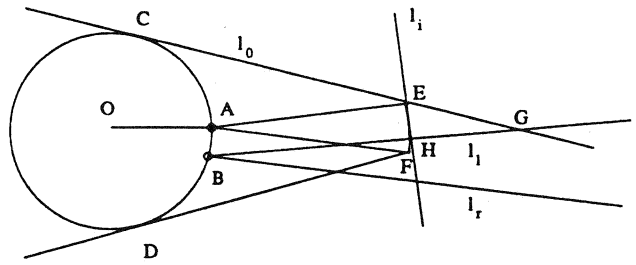

Figure 3: Set 1 Distances

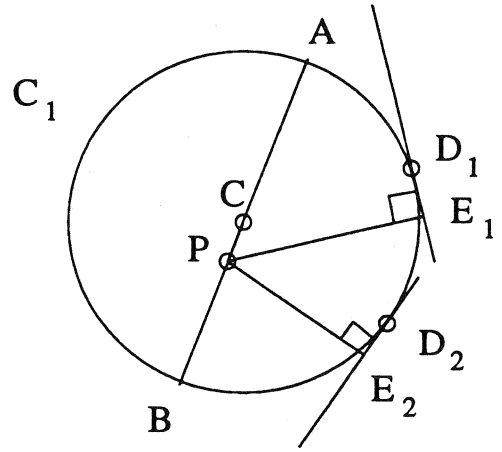

Figure 4: Set 2 Distances

reading after rotating the sonar sensor about the origin by an amount less than $\angle AEC$ (call that angle α) to the new position B. The sonar range distances from B to the lines in sets $S1$, $S2$, and $S3$ are monotonically decreasing, which permits a simple determination of the line that produced r.

Now, consider a clockwise rotation of angle θ of the sonar located at A rotated about O from A to B where $0 < \theta < \alpha$ (see Figure 3). Any ray in the second sonar scan to the right of l_l will intersect all lines in $S1$ at a greater distance than l_l will. In addition, the distance along l_l monotonically decreases to a line l as it starts at line l_0 and is rotated about E to line l_i. To see this, drop a perpendicular from E to segment $\overline{HG}$ of height $h = d \times \sin(\beta)$ (where $d = |\ \overline{EH}\ |$, and β is $\angle EHG$). It is clear that as segment $\overline{EG}$ rotates clockwise around E, segment $\overline{HI}$ goes monotonically to length zero, where point I is the intersection of lines l_i and l. (Note that the perpendicular to l_l through E is past l_i.) This follows from the fact that if $b = |\ \overline{HI}\ |$, then the area of triangle $\triangle EHI$ monotonically decreases, so that $\frac{1}{2}bh$ does, too, which implies that b does since h is constant.

Now, to show that the distance from B to the tangent lines along the circular arc EF decreases monotonically, consider the more general case shown in Figure 4. Given a circle, C_1, of radius r and a point, P, in the circle not at the center, C, then the minimum distance from P to a tangent line of the circle is maximum to the tangent line at A. It is minimum

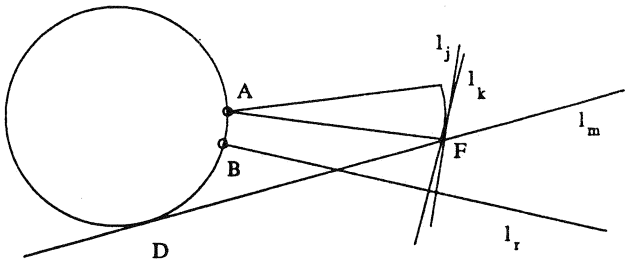

Figure 5: Set 3 Distances

to the tangent line at B, and monotonically decreases to the tangent line at D as point D moves from A to B along the circle.

First, let's show that the distance decreases monotonically. Suppose not; then there exist two points D_1 and D_2 on the circle between A and B such that P is equidistant from the tangent lines to circle C_1 at D_1 and D_2 (let E_1 and E_2 be the points of intersection of the perpendiculars to the tangent lines at D_1 and D_2, respectively). Then there is a circle, C_2, centered at P of radius $|\ \overline{PE_1}\ |$ such that there are two lines tangent to the two circles C_1 and C_2 on the same side of line $\overleftrightarrow{AB}$. $\otimes$

This applies directly to all points along arc EF in Figure 3 since at no point Q along this arc is $\overline{BQ}$ perpendicular to the tangent at Q (this can't be since $\overline{AQ}$ is perpendicular to the tangent line there). Thus, the claim holds for the set $S2$.

Now, for the final set of lines, $S3$, we consider two subsets (see Figure 5). Let l_k be the line between l_j and l_m which is perpendicular to l_r. Then, for all lines between l_k and l_m, as l_k is rotated around F to l_m, the shortest distance from B to the line is along a line clockwise from l_r; therefore, for those lines the shortest distance in the sonar wedge from B is along line l_r and monotonically decreases.

Finally, for the lines from l_j to l_k, we claim that the shortest distance from B decreases monotonically. Suppose not. Then there exist two points J_1 and J_2 such that the distance d to B is the same. Since for this set of lines, the shortest distance is on the perpendicular to B, then there exist two tangent lines to the circle centered at B of radius d such that both lines go through F and are on the same side of the circle. $\otimes$

Thus, we have shown that given the set of lines that could cause a sonar return of r from a single wall, then a second sonar return from a rotated location is sufficient to disambiguate the pose of the wall. However, the proof has imposed two conditions on the rotated position:

- The angle between the first and second sonar locations cannot exceed α, the angle between the lines l_0 and $\overleftrightarrow{AE}$ (Figure 3).

- The line $\overleftrightarrow{BA}$ (Figure 4) should not cut the arc EF (Figure 3).

2 Computational Scheme

This approach assumes that a single flat surface gives rise to the sonar readings. All surface hypotheses determined by the method must be subsequently verified. A computational scheme to determine the best estimate of the line l (the projection of the flat surface into the robot's sensor ring plane) is very easily developed based on the above proof (the terminology below is with reference to Figure 2):

Pose Recovery Algorithm

1. Get first sonar reading, r_1.
2. Determine $\angle AEC$ ($\overline{AE} = r_1$).
3. Rotate sensor clockwise $\theta°$ about O, where $\theta < \angle AEC$.
4. Get second sonar range reading, r_2.
5. Use bisection search to find the line $l \in S1 \bigcup S2 \bigcup S3$ such that the sonar distance from B to l is closest to r_2.

A complete technical description of this method can be found elsewhere[6].

3 Practical Considerations

In practice, robots are seldom confronted with a single wall, and, of course, sonars do not get reflections off walls at too small an angle. We describe here our experimental setup and the details for exploiting the theory given above.

3.1 Synthetic Data

We have applied the computational scheme to recover the pose of the line from two sonar readings. In the following tests, a set of lines taken from the sets $S1$, $S2$, and $S3$ are generated, and the Pose Recovery Algorithm used to recover a corresponding line. In order to compare the results with the originals, we have plotted the difference in their (ρ, θ) parameters (ρ is the shortest distance from the origin to the line, and θ is the angle the line makes with the x-axis). Figures 6-12 give the results for walls placed at a range of 500mm and 2000mm, respectively. Basically, the method consists of producing the curve associated with the first sonar reading (e.g., Figure 7), then inverting the curve and finding the line corresponding to the distance given by the second range reading.

As can be seen, these are very accurate results. There should be no error at all in these results, and the error shown is due to numerical errors in computing the sonar range to a line and the distance from the second sonar sensor location to the lines in sets $S1$, $S2$, and $S3$. As can be seen from the plots, the largest error is associated with the lines farthest from the direction of the second sonar direction.

3.2 Polaroid Data

Here we demonstrate the results of the method on some actual Polaroid data on an actual wall located 500mm and 2000mm

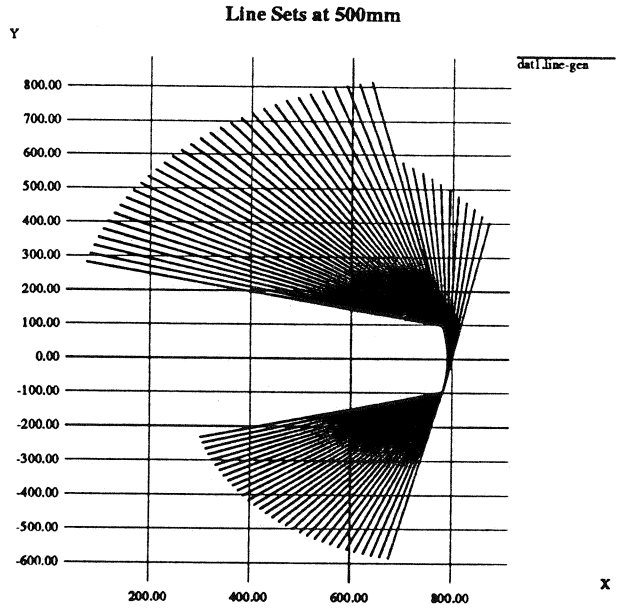

Figure 6: Possible Lines which Generate a Return at 500mm

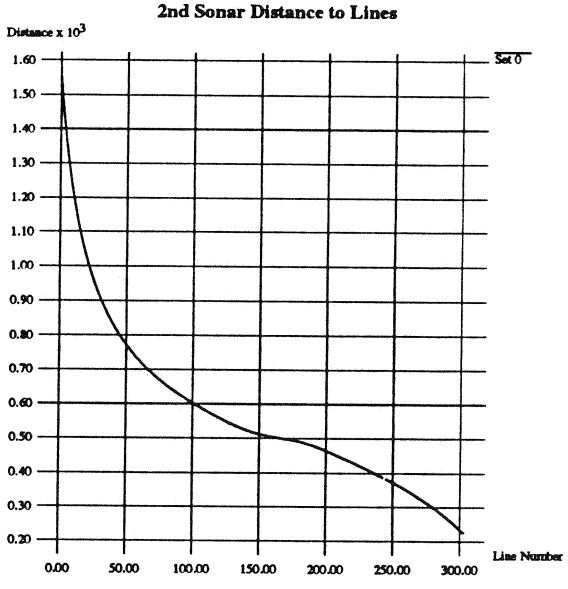

Figure 7: Second Sonar Distance Function for 500mm

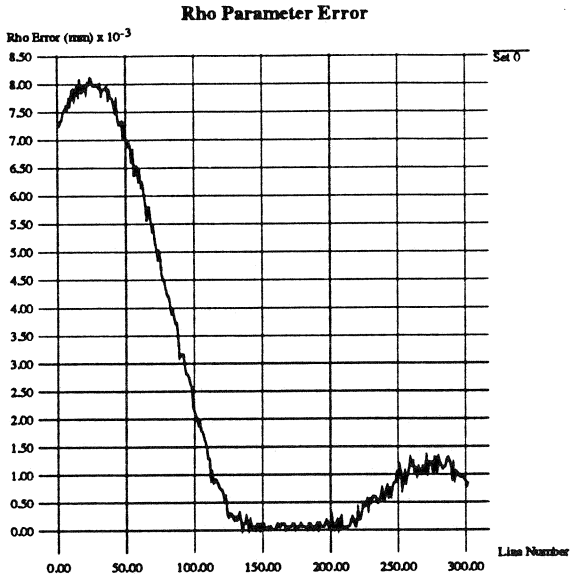

Figure 8: Error in ρ Parameter of Lines at 500mm

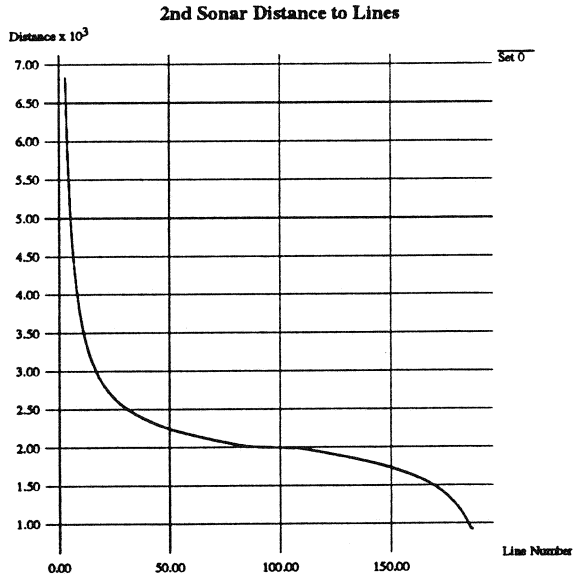

Figure 10: Second Sonar Distance Function for 2000mm

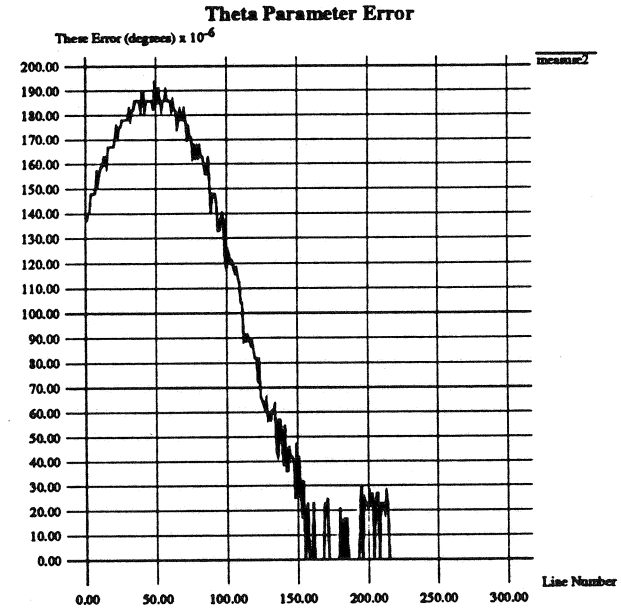

Figure 9: Error in θ Parameter of Lines at 500mm

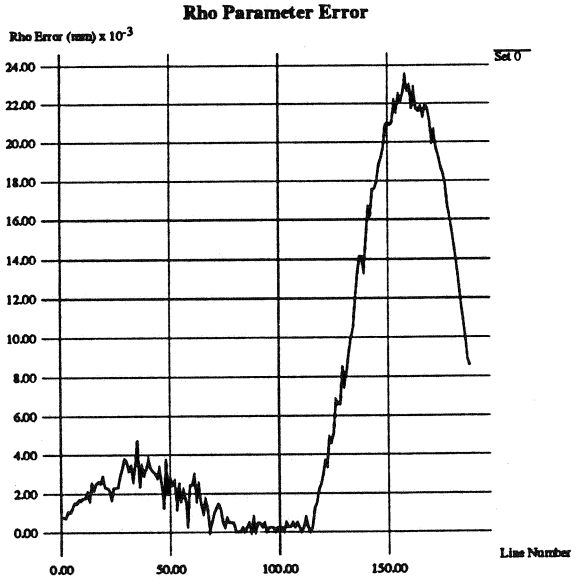

Figure 11: Error in ρ Parameter of Lines at 2000mm

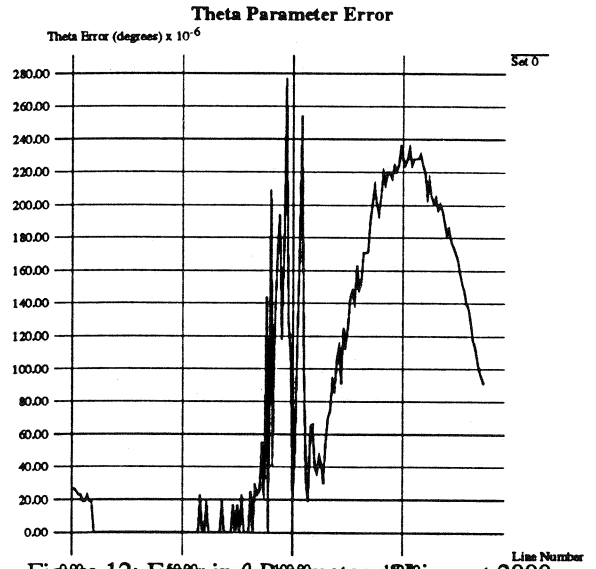

Figure 12: Error in θ Parameter of Lines at 2000mm

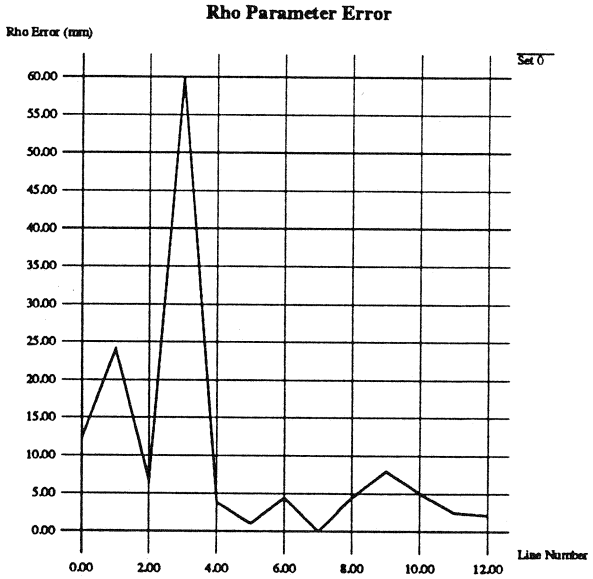

Figure 13: Error in ρ Parameter of Actual Line at 500mm

in front of the mobile robot. Figures 13- 16 show the results.

4 Discussion

We have presented a solution to the 1W1S problem, and believe that it is optimal. We have demonstrated its effectiveness on synthetic data, and on actual Polaroid sonar data. In other experiments [5] we have shown that the line estimates for two range sensor readings produced by this method are better than using line estimates from the two points obtained simply from using the sensor orientation and range in that direction (as suggested by e.g., see[8]: "A sonar map is generated by placing a dot at the computer range along the transducer orientation").

The error in the actual data is due to both the error in the range readings and the numerical error involved in the computation. The minimum incident angle does not need to be accounted for since the method only produces a flat surface hypothesis for two neighboring sonar sensors that both produce a range value. For more details see[6].

Given that the smallest angle that gives a sonar return is about 60 degrees, it is necessary to have at least 20 sonar sensors equally spaced and no more than 18 degrees apart in order to be able to detect a wall within sonar range of a mobile platform. Our particular Labmate has a 24 sonar ring with sensors spaced 15 degrees apart and was used for the experiments described here. The idea is that this method permits the hypothesis on any possible walls, and then those hypotheses can be checked out by moving and taking more readings.

We are also studying the $k\mathrm{W}m\mathrm{S}$ problem in more generality. We believe that the equations and specific constraints can be solved in the multiple wall, multiple sonar case as well.

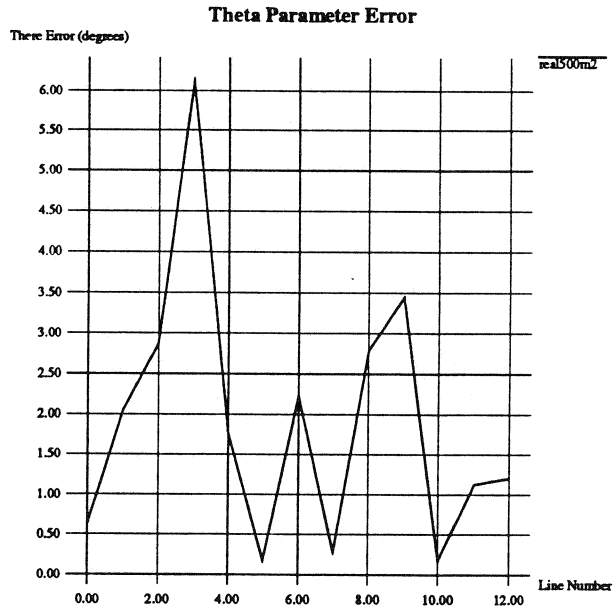

Figure 14: Error in θ Parameter of Actual Line at 500mm

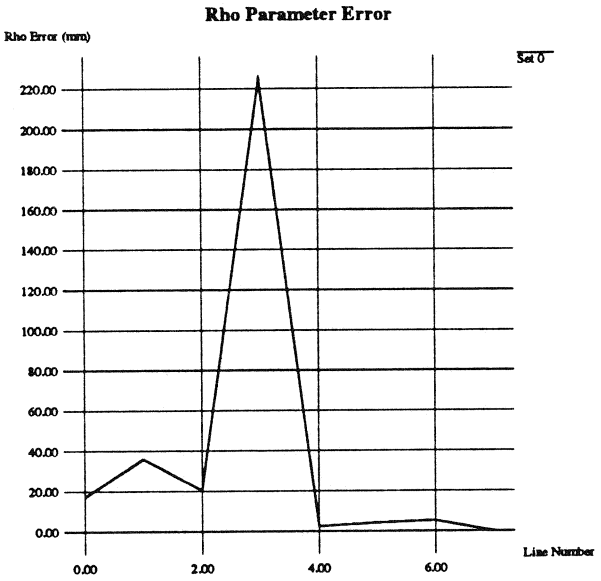

Figure 15: Error in ρ Parameter of Actual Line at 2000mm

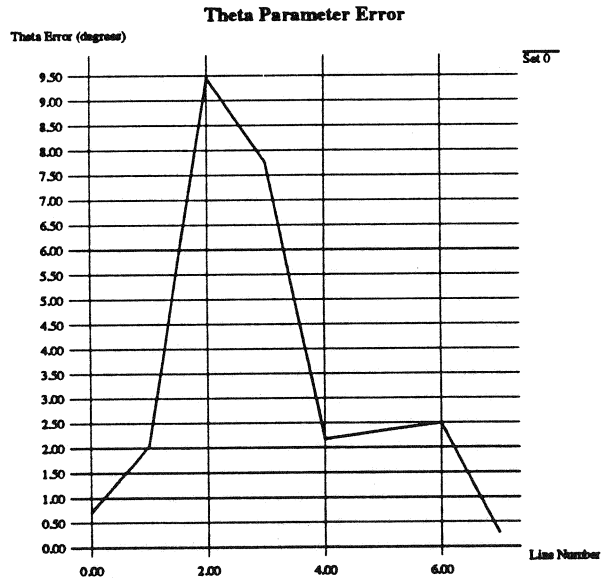

Figure 16: Error in θ Parameter of Actual Line at 2000mm

References

[1] B. Bozma and R. Kuc. Differentiating sonar reflections from corners and planes by employing an intelligent sensor. *IEEE Trans. Pattern Analysis and Machine Intelligence*, 12(6):pp. 560–569, June 1990.

[2] O. Bozma and R. Kuc. Building a sonar map in a specular environment using a single mobile sensor. *IEEE Trans. Pattern Analysis and Machine Intelligence*, 13(12):pp. 1260–1269, December 1991.

[3] J. Crowley. Navigation for an intelligent robot. *IEEE Journal of Robotics and Automation*, RA-1(1):pp. 31–41, March 1985.

[4] A. Elfes. Sonar-based real-world modeling and navigation. *IEEE Trans. Robotics and Automation*, RA-3(3):pp. 249–265, June 1987.

[5] Thomas C. Henderson, Mohamed Dekhil, Beat Bruderlin, L. Schenkat, and L. Veigel. Flat surface recovery from sonar data. In *DARPA Image Understanding Workshop*, page to appear, February 1996.

[6] Thomas C. Henderson, Mohamed Dekhil, Beat Brüderlin, L. Schenkat, and L. Veigel. The *kwms* problem. Technical Report UUCS-96, University of Utah, March 1996.

[7] L. Kleeman and R. Kuc. An optimal sonar array for target localization and classification. *IEEE Trans. Robotics and Automation*, 14(4):pp. 295–318, August 1995.

[8] R. Kuc. A spatial sampling criterion for sonar obstacle detection. *IEEE Trans. Pattern Analysis and Machine Intelligence*, 12(7):pp. 686–690, July 1990.

[9] R. Kuc. A physically based navigation strategy for sonar guided vehicles. *Int. J. Robotics Research*, 10(2):pp. 75–87, April 1991.

[10] Larry Matthies and A. Elfes. Integration of sonar and stereo range data using a grid-based representation. In *IEEE Int. Conf. Robotics and Automation*, pages pp. 727–733, April 1988.

[11] Herbert Peremans, K. Audenaert, and Jan Van Campenhout. A high-resolution sensor based on tri-aural perception. *IEEE Trans. Robotics and Automation*, 9(1):pp. 36–48, February 1993.